

Study of antiferroelectric ammonium dihydrogen phosphate (ADP) by pulsed NMR*

S. R. Kasturi[†] and P. R. Moran

Physics Department, University of Wisconsin, Madison, Wisconsin 53706

(Received 29 January 1975)

Proton NMR relaxation rates have been measured in ammonium dihydrogen phosphate (ADP) over a temperature range from 315 to 74°K. The longitudinal lab-frame relaxation rate $1/T_1$ is completely dominated by the thermally activated hindered rotations of the ammonium ions. At the antiferroelectric phase transition, $T_c \simeq 147^\circ\text{K}$, $1/T_1$ exhibits a 50% discontinuity and, for $T < T_c$, develops a temperature-dependent anisotropy. The rotating-frame relaxation rates, $1/T_{1\rho}$, show not only an expected smoothly temperature-dependent baseline contribution associated with the same ammonium-ion reorientations which dominate $1/T_1$, but also some additional sharply temperature-dependent structures. Weak structures in $1/T_{1\rho}$ near room temperature appear due to impurity-diffusion effects and can be eliminated by annealing the ADP samples. More interesting is an extremely strong ($\sim 5 \times 10^2 \text{ sec}^{-1}$) intrinsic phase-transition anomaly contributing to $1/T_{1\rho}$ for temperature very close to T_c . Analysis of the quantitative results indicates that (i) the ammonium ions reorient by two-fold rotations both above and below T_c . (ii) There is NMR evidence for severe ammonium-ion distortions and rotational anisotropies in the antiferroelectric state, but the phase transition itself does not involve cooperative rotational ordering of the ammonium ions. (iii) Critical slowing of some dynamical mechanism is strong reflected in the $1/T_{1\rho}$ anomaly near the phase transition; the associated correlation times become very long, $\sim 10^{-6}$ sec, for temperatures just above T_c and rapidly freeze-in to an essentially static behavior for temperatures below T_c .

I. INTRODUCTION

This paper reports a study of proton NMR spin-lattice relaxation times for the hydrogen-bonded antiferroelectric ammonium dihydrogen phosphate. Both laboratory-frame T_1 and rotating-frame $T_{1\rho}$ times were measured over a temperature range from 330 to 74°K.

Ammonium dihydrogen phosphate, $\text{NH}_4\text{H}_2\text{PO}_4$ (ADP), belongs to the family of isomorphous hydrogen-bonded ferroelectrics of the potassium dihydrogen phosphate KH_2PO_4 (KDP), type. It undergoes a phase transition from paraelectric (PE) to antiferroelectric (AFE) state at 148°K. ADP has tetragonal structure in the PE phase and orthorhombic in AFE phase. Complete descriptions of the crystallography of the PE phase have been investigated by various authors, e.g., x-ray analyses were made by Ueda¹ and by Keeling and Pepinsky,² neutron-diffraction analysis by Tenzer *et al.*,³ and an electron-diffraction study was made by Kolomiichuk.⁴ Large ADP crystals shatter upon first cooling through the phase transition, resulting in perpendicular twinned crystals with random perpendicular orientations along the a and b axes. For this reason, the antiferroelectric structure has been investigated only by x-ray diffraction,^{2,5} which indicates the a or b axis as the antiferroelectric axis. In the absence of detailed neutron-diffraction studies, the ordering of the hydrogen bonds in ADP is assumed to be that proposed theoretically by Nagamiya⁶ and by Mason and Matthias.⁷

Measurements of the ADP dielectric constants,⁷ specific heat,⁸ and infrared absorption⁹ all support

this theoretical model that the antiferroelectric ordering involves the protons in the hydrogen bonds linking the acid groups (H_2PO_4). The specific-heat anomaly at the transition temperature T_c indicates a first-order phase transition, and together with a large isotope effect on T_c for deuterated samples, implies that the hydrogen-bond motions dominate the phase-transition dynamics. This is also supported by high-pressure dielectric-constant^{10,11} studies. On the other hand, the ir studies⁹ show strong ammonium-ion distortions occurring at T_c , suggesting that the ammonium-ion motions coupled together with the acid-group proton motions govern the phase-transition dynamics.

Magnetic-resonance relaxation measurement provides a powerful tool for studying the dynamical behavior of atomic systems. Both electron resonance¹² and nuclear resonance¹³ have been used to study the dynamics in hydrogen-bonded ferroelectrics. NMR proton relaxation times T_1 have been measured as a function of temperature in ADP powders using cw techniques by Newman¹⁴ and in oriented samples using pulsed techniques by Genin *et al.*¹⁵ These two sets of NMR data differ significantly from one to another. In the experimental reported here, we measured both the proton lab-frame relaxation rates $1/T_1$ and the rotating-frame rates, $1/T_{1\rho}$.^{16,17} The rate $1/T_{1\rho}$ is the relaxation rate of nuclear-spin magnetization which is initially aligned along the Larmor rotating component H_1 of a resonant rf magnetic field. The $1/T_{1\rho}$ studies are particularly useful because (i) $1/T_{1\rho}$ remains sensitive to much slower fluctuations than does $1/T_1$, (ii) $1/T_{1\rho}$ is sensitive to an additional class

of local-field fluctuations which do not contribute the $1/T_1$ behavior, (iii) when both relaxation rates $1/T_1$ and $1/T_{1p}$ are dominated by rapid hundred rotation of the ammonium ions, then the ratio T_1/T_{1p} depends upon the type of rotation occurring.

II. EXPERIMENTAL APPARATUS AND PROCEDURE

The NMR measurements were made using an 8-MHz pulsed phase-coherent NMR crossed-coil spectrometer and a field-regulated Magnion 12-in. electromagnet. The proton free-induction-decay (FID) signal, after phase sensitive detection, was averaged by a box-car integrator over as many repetitions as practical depending on the length of the spin-lattice relaxation times. Detailed descriptions of the spectrometer, the sample probe construction, the cold-gas flow temperature regulation system, and Dewar assembly are given elsewhere.^{18,19} The over-all thermal range was from 330 to 74 °K; temperatures below liquid nitrogen, 77 °K, were obtained by bubbling cold helium gas through liquid nitrogen to produce additional cooling. The temperature difference measured across a 1-cm³ sample was less than 0.2 °K. The temperature stability from room temperature down to about 105 °K was ± 0.05 °K and the temperature accuracy estimated at about 0.3 °K. For temperatures below 105 °K and above room temperature, system performance grew worse approaching temperature stabilities and uncertainties of ± 1 °K at the extreme temperatures.

The samples were cut to about $1 \times 1 \times 1$ cm³ from Harshaw optical grade Z-cut ADP crystals. The samples were lightly coated with Duco cement so that even upon shattering during the first cooling through T_c the crystallite alignment is maintained. For the several samples used, the data were highly reproducible from sample to sample, except in the temperature range close to room temperature due to impurity diffusion effects to be discussed later.

For temperatures above 100 °K, T_1 was measured by the 180°–90° pulse method and below 100 °K, by the 90° pulse method. Typical uncertainty in T_1 was about $\pm 2\%$ while occasionally, slightly larger errors were encountered.

The spin-lattice relaxation times in the rotating frame T_{1p} were measured by the Slichter–Ailion techniques.^{20,21} The magnetization is locked along the rf field H_1 by adiabatic passage to resonance. The size of the magnetization M_x is then measured as a function of the duration t of the rf pulse. The T_{1p} values were obtained by a least-squares fit of the data to the relation $\ln[M_x(t)/M_x(0)] = -t/T_{1p}$. Typical errors in the T_{1p} are about $\pm 5\%$, while sometimes errors as much as $\pm 10\%$ have resulted. An H_1 of about 5.6 G was used in these T_{1p} measurements, which is about twice the local dipolar field ($H_L \sim 2.75$ G). The large intra-ammonium

dipolar interactions are completely motionally narrowed in this temperature range.

III. THEORETICAL BACKGROUND

A. Ammonium-ion rotation

Except close to the phase-transition temperature, both the $1/T_1$ and $1/T_{1p}$ proton relaxation rates are dominated^{14,15} by the ammonium-ion hindered rotation, which causes fluctuations of the large (~ 7 G) intra-ammonium dipole-dipole interactions. For temperatures above 90 °K, the rotational correlation time remains small compared with the rigid lattice T_2 . In this motionally narrowed limit, the two classes of ADP protons (the ammonium protons and the acid, hydrogenbond, protons) can maintain a common spin-temperature and relax at a common rate. Furthermore, in this limit, the measured rotating-frame relaxation rate $1/T_1$ induced by the ammonium-ion rotation is physically identical to the motionally narrowed intra-ammonium contribution to the system $1/T_2$. Consequently, both $1/T_1$ and $1/T_{1p}$ can be interpreted according to a standard perturbation-theory approach, as detailed, for example, by Abragam²² in his treatment of relaxation by molecular rotation in liquid and gases.

Abragam shows how the dipole-dipole rotational correlation functions may be calculated by expanding the angular probability function in spherical harmonics, and gives a specific evaluation for the case of diffusional rotation through infinitesimal angles. We have extended this same formalism to the case of protons on the ammonium tetrahedra in the ADP lattice, where the reorientation occurs via rotation through finite angles. The specific derivations and several numerical calculations for various rotational mechanisms are very straightforward, exactly paralleling the examples detailed in Abragam's book. These full calculations, however, are not necessary for understanding the basics of the observed relaxation behavior and are far too lengthy to include in the present paper.

An outline of the derivations of theoretical expressions relating to $1/T_1$ and $1/T_{1p}$ is given in the Appendix with the chief results summarized below. In the following, γ is the proton gyromagnetic ratio, H_0 is the externally applied static field, and H_1 is the Larmor rotating component of the rf magnetic field.

1. The relaxation rates depend upon a rotational correlation time τ_r

In the two limits $2\gamma H_0 \tau_r \gg 1$ and $\gamma H_0 \tau_r \ll 1$, the inverse of τ_r is given simply by the sum of mean rotational jump rates for each independent axis of molecular reorientation. For example, the three two-fold rotational axes pass through the center

nitrogen position and the opposite edges of the tetrahedron whose corners are the proton positions. These two-fold axes lie, on the average, essentially along the ADP-crystal a , b , and c axes. For two-fold rotational reorientation

$$1/\tau_r = 1/\tau_a + 1/\tau_b + 1/\tau_c, \quad (1)$$

where $1/\tau_a$, $1/\tau_b$, and $1/\tau_c$ are the mean two-fold (180° rotation) jump rates about the respective rotational axes.

2. *The tetrahedral symmetry of the proton positions is sufficient that that form given by Eq. (1) is independent of the orientation of the external magnetic field with respect to the crystal axes*

A similar result is obtained for all modes of reorientation, three-fold (120°), 90° rotations, infinitesimal rotations, etc. Consequently, according to the discussion following Eq. (A11) in the Appendix and Eqs. (A17) and (A18), there would be no relaxation rate anisotropy.

Our experiments, however, reveal a strong T_1 anisotropy in the AFE phase. This can occur if the ammonium-ion tetrahedron is distorted in the AFE phase; strong distortions of this kind have already been observed through their effect on the ir absorption,⁹ for example, for twofold rotations where some distortions greatly increase the relative dipolar interaction of the proton pairs whose internuclear axes are perpendicular to the crystal c axis. Equations (A19) and (A20) give

$$1/\tau_r = \frac{1}{4}(2/\tau_a + 2/\tau_b), \quad (2)$$

for H_0 parallel to the c axis, and

$$1/\tau_r = \frac{1}{4}(2/\tau_c + 1/\tau_a + 1/\tau_b), \quad (3)$$

for H_0 perpendicular to the c axis.

3. *Approximate expressions for $1/T_1$, which are correct for $\gamma H_0 \tau_r \gg 1$ and $2\gamma H_0 \tau_r \ll 1$, but inexact for intermediate τ_r values, can be derived*

For two-fold ammonium-ion rotations, the result from Eqs. (A8) and (A16) is

$$1/T_1 \approx \frac{3}{2}(\gamma H_1)^2 \tau_r [1 + (1.6 \gamma H_0 \tau_r)^2]^{-1}, \quad (4)$$

where τ_r is given by Eq. (1), and H_1^2 is the proton local-field second moment from the intra-ammonium dipolar interactions. Equation (4) yields a minimum T_1 , using a calculated¹³ proton second moment of 42 G^2 , of

$$T_{1 \text{ min}} \approx 4.1 \times 10^{-3} \text{ sec}. \quad (5)$$

4. *For $2\gamma H_0 \tau_r \ll 1$, $1/T_{1\rho}$ is proportional to $1/T_1$, as discussed prior to Eq. (A10) in the Appendix*

If reorientation occurs by two-fold rotations, and if the ammonium ion suffers a 5% tetragonal distortion in the ADP tetragonal lattice, a remark-

able result occurs: $1/T_{1\rho}$ is actually smaller than $1/T_1$, their ratio being 0.7. For three-fold or infinitesimal rotations, $T_1 = T_{1\rho}$, independent of any distortions.

5. *For $\gamma H_0 \tau_r \gg 1$, but $\gamma H_1 \tau_r \ll 1$, $1/T_{1\rho}$ continues to grow proportionally to τ_r*

The Appendix shows the contribution from intra-ammonium tetrahedral interactions vanishes, as expressed in Eq. (A13). There remain, however, the inter-ammonium and proton-phosphorous interactions. These contributed a mean-squared local field approximately 10% that of the intra-ammonium interactions. The short-correlation-time limit of Eq. (A10) then gives

$$1/T_{1\rho} \approx \frac{3}{2}(\gamma H_1)^2 (0.1) \tau_r. \quad (6)$$

B. Other interactions

In addition to the ammonium hindered rotation contributions to $1/T_{1\rho}$ discussed above, we observe experimentally, in certain temperature ranges, other contributions as well. Without a detailed knowledge of the mechanisms responsible, we parametrize each of these other interactions simply by a mean-squared field fluctuation h^2 and a characteristic correlation time τ . Assuming that $h^2 \ll H_1^2$, a simple expression for the contribution to $1/T_1$ is given in Eq. (A10),

$$1/T_\rho = \gamma^2 h^2 \tau [1 + (\gamma H_1 \tau)^2]^{-1}. \quad (7)$$

Typically, we find a temperature dependence described by a thermally activated τ ,

$$\tau = \tau_0 e^{E/kT}. \quad (8)$$

IV. EXPERIMENTAL T_1 RESULTS

Our results for the ADP proton T_1 are shown in Fig. 1. For clarity of the figures, the data points drawn in on Fig. 1 represent only about 25% of the T_1 data actually acquired. As described by Eq. (4), T_1 shows a minimum when $(1.6)\gamma H_0 \tau_r = 1$; this is familiarly called a "BPP minimum." The BPP minimum we observe at $\sim 150^\circ \text{K}$ with an 8-MHz spectrometer is consistent with the higher temperature ($\sim 170^\circ \text{K}$) minimum observed by Newman¹⁴ at 30 MHz and by Genin *et al.*¹⁵ with 42-MHz pulsed measurements. Our results, in agreement with those of Genin *et al.*, do not show the high-temperature secondary minimum seen in Newman's cw experiments, but do reveal a marked discontinuity in T_1 at the transition temperature $T_c \approx 148^\circ \text{K}$.

The discontinuity in T_1 at T_c is not attributable to the physical shattering of the crystal. We have performed heating and cooling cycle experiments from 15 above to 15°K below T_c , measuring T_1 on intervals of about 0.5°K . Within the experimental reproducibility of sample temperature, we observe no hysteresis effects, and the T_1 jumps from 2.9

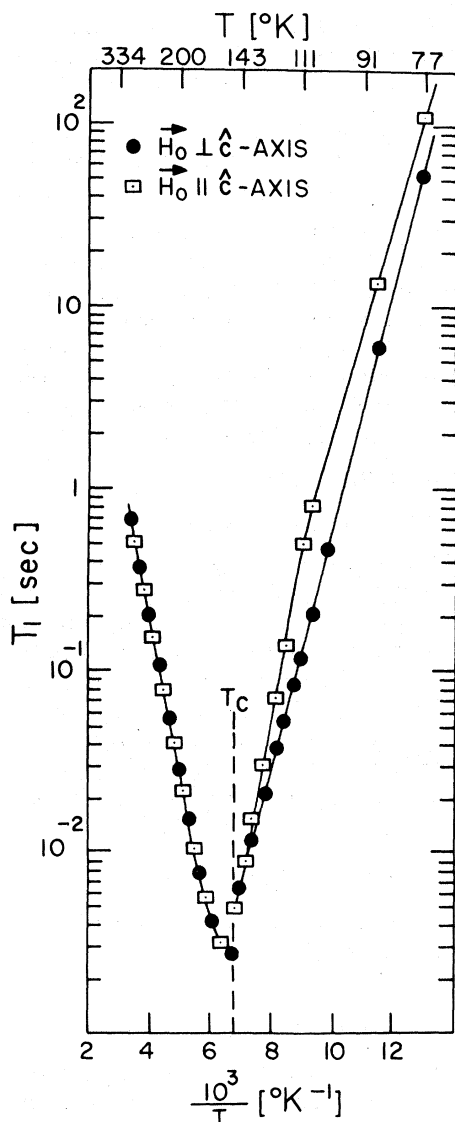


FIG. 1. Temperature dependence of the proton NMR longitudinal relaxation time T_1 in ADP.

to 4.7 msec over a temperature interval less than $\pm 0.25^\circ\text{K}$.

We measure a minimum T_1 of 2.7 msec at 150°K . The minimum T_1 estimated theoretically in Eq. (5), is 4.1 msec. Considering the influence of other dipolar interactions, e.g., proton-phosphorus, and large uncertainties in calculating the exact intra-ammonium second moments, the predicted and measured T_1 's are in quite good agreement.

As shown in Fig. 1, we observe a single isotropic thermally-activated behavior for T_1 in the PE phase. In the AFE phase, however, we observe a temperature-dependent anisotropy. We have performed a least-squares fit of $\ln(1/T_1)$ vs $1/kT$ to obtain the activation energies for the re-

laxation rates.

(i) In the PE phase, there is no anisotropy and we find a single activation energy,

$$E = 3.77 \pm 0.05 \text{ kcal/mole} . \quad (9)$$

This agrees well with the Genin *et al.* value of 3.7 ± 0.3 kcal/mole.

(ii) In the AFE phase, there is a marked anisotropy. The observed anisotropic behavior can be described by the $\gamma H_0 \tau_r \gg 1$ limit of Eq. (4) together with the expressions for τ_r given by Eqs. (5) and (6), where

$$\tau_c = \tau_0 e^{E_c/kT} , \quad (10)$$

$$\tau_a = \tau_b = \tau_0 e^{E_a/kT} . \quad (11)$$

The activation energies found are

$$E_c = 4.1 \pm 0.2 \text{ kcal/mole} \quad (12)$$

and

$$E_a = 2.8 \pm 0.2 \text{ kcal/mole} . \quad (13)$$

We stress that the theoretical prediction of an anisotropy assumes both a severe ammonium distortion and reorientation by two-fold rotations, i. e., 180° reorientations about axes perpendicular to the tetrahedron edges. Three-fold rotations, i. e., reorientations occurring about axes corresponding to the proton-nitrogen internuclear vector, even assuming a distorted ammonium configuration, do not yield an anisotropy. As discussed later, the T_{1p} measurements in the short-correlation limit are also consistent only with two-fold hindered rotation of the ammonium ion.

Thus, the experimental results together with calculated $1/T_1$ behavior for relaxation via hindered ammonium-ion reorientation give the following picture. The ammonium ions reorient by the three two-fold rotations occurring essentially about the three crystal axes. The mean rotation times τ_a , τ_b , and τ_c are thermally activated, as described by Eq. (8). The pre-exponential factor τ_0 can be estimated in the PE phase from our data,

$$\tau_0 = 2 \times 10^{-14 \pm 0.5} \text{ sec} . \quad (14)$$

This value agrees quite well with calculated values by O'Reilly and Tsang²³ for either two or three-fold rotations. In the PE phase, τ_a , τ_b , and τ_c all have essentially the same activation energy, about 3.8 kcal/mole, as given in Eq. (6). In the AFE phase, the two-component activation behavior combined with the anisotropy in $1/T_1$ suggests a severely distorted ammonium-ion configuration. This distortion is also implied by previous ir measurements.⁹ The observed $1/T_1$ behavior in the AFE phase further suggests that in the phase transition, the activation energy for τ_c increases from the PE

value of 3.8 kcal/mole to the value of about 4.1 kcal/mole given in Eq. (7). At the same time, τ_a and τ_b exhibit a decrease in activation energy to a value of about 2.8 kcal/mole.

Although there is a T_1 discontinuity at T_c , the fractional change in $1/T_1$ is only about 50%. This implies similar changes in the rotational correlation times. Such a small change, while consistent with an ammonium-ion distortion and changes in lattice structure, appears to rule out the possibility that cooperative rotational ordering²⁴ of the ammonium ions is involved in the AFE phase transition.

V. EXPERIMENTAL $T_{1\rho}$ RESULTS

For the $T_{1\rho}$ measurements reported here, H_0 is perpendicular to the c axis (parallel to the a axis in the PE phase), and H_1 is 5.6 G. The residual unarrowed rms local field is approximately 3 G from 300 to 100 °K, and the line-breadth angular dependence is available from the work of Adriaenssens and Bjorkstam.²⁵ The solid line curve in Fig. 2 shows the observed $T_{1\rho}$ behavior from 315 to 74 °K. For clarity in presenting the figure, the actual data points are not shown. The T_1 data, through which the curve in Fig. 2 was drawn, were taken at temperature intervals of approximately 5 °K in the ranges where $T_{1\rho}$ was smoothly varying. Near room temperature and near T_c , where $T_{1\rho}$ exhibits structured effects, the data were taken at temperature intervals of (2–3)°K. For comparison, the T_1 behavior is given by the dotted-line curve, which has been displaced upwards by a factor of 2 for clarity in the drawing.

Apart from the weak $1/T_{1\rho}$ structures near room temperature and the strong $1/T_{1\rho}$ structure occurring very close to T_c , the remaining $1/T_{1\rho}$ behavior appears relatively simple. That is, for $T > T_c$, $T_{1\rho}$ decreases in proportion to T_1 , as discussed theoretically in part C4. of Sec. III. For $T < T_c$, $T_{1\rho}$ continues to decrease, as described by Eq. (6) for a continuing increase of τ , with decreasing temperature. In the range $135^\circ\text{K} > T > 80^\circ\text{K}$, $T_{1\rho}$ is unmeasurably short with our present apparatus. As indicated by the dot-dashed line, however, $T_{1\rho}$ passes through rotating-frame minimum ($\gamma H_1 \tau_r \sim 1$) somewhere near 100 °K. At 80 °K, $T_{1\rho}$ again becomes measurably long and increases rapidly with decreasing temperature to our lower limit of 74 °K. This behavior supports our model that both $1/T_1$ and $1/T_{1\rho}$ are, over most of the temperature range investigated, dominated by the thermally activated rotations of the ammonium ions.

The relative simplicity of this base-line behavior, described above for $T_{1\rho}$ in ADP, contrasts sharply with exceedingly complex behavior measured by Grosescu²⁶ for NMR dipolar-relaxation-

time experiments in ammonium dihydrogen arsenate (ADA). New information on the dynamics of ADP comes from a detailed investigation of the sharply temperature-dependent $1/T_{1\rho}$ structures shown in Fig. 2. The strong anomaly occurring at T_c in the vicinity of 150 °K is related to the phase-transition dynamics. The relatively weaker structures above 250 °K in the vicinity of room temperature appear to be related to nonintrinsic impurity and defect-state effects.

The $T_{1\rho}$ and T_1 data from 315 to 250 °K are shown in Fig. 3. The open and closed circles show, respectively, $T_{1\rho}$ before and after thermal annealing of the ADP samples; the triangles show T_1 . The open circles show that, before annealing the sample, two shallow minima in $T_{1\rho}$ appear at 290 and 270 °K. Interpreted according to Eqs. (7) and (8) of Sec. III, we find activation energies of approximately 6 ± 0.5 kcal/mole and 8.5 ± 0.5 kcal/mole for the 270 and 290 °K features, respectively. For both, the pre-exponential factors τ_0 in Eq. (7), are estimated at about 10^{-9} – 10^{-10} sec. From the actual values of $1/T_{1\rho}$, we estimate the mean-squared field fluctuations as $h^2 \approx 10 \times 10^{-4}$ G². The large values for τ_0 and the activation energies, and the small values of h^2 , suggest that the relaxation mechanism is diffusion of a small concentration (~ 100 ppm) of grown-in defects or impurities.

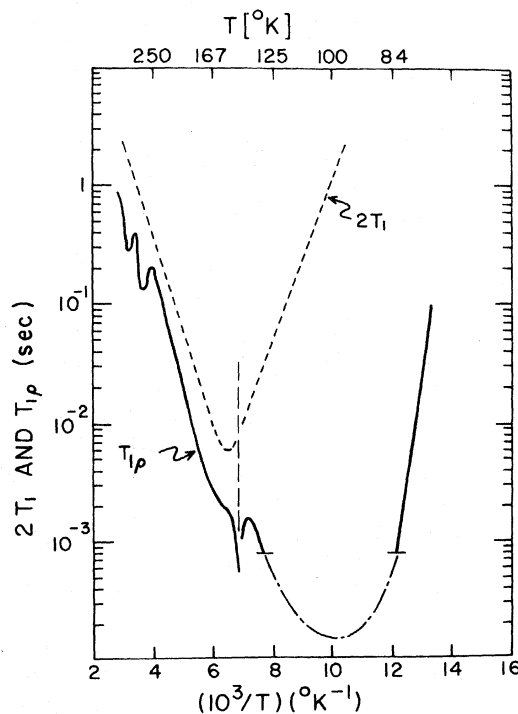


FIG. 2. Overall temperature dependence of the rotating-frame relaxation time, $T_{1\rho}$, shown by the solid curve, and comparison with T_1 by the dotted curve.

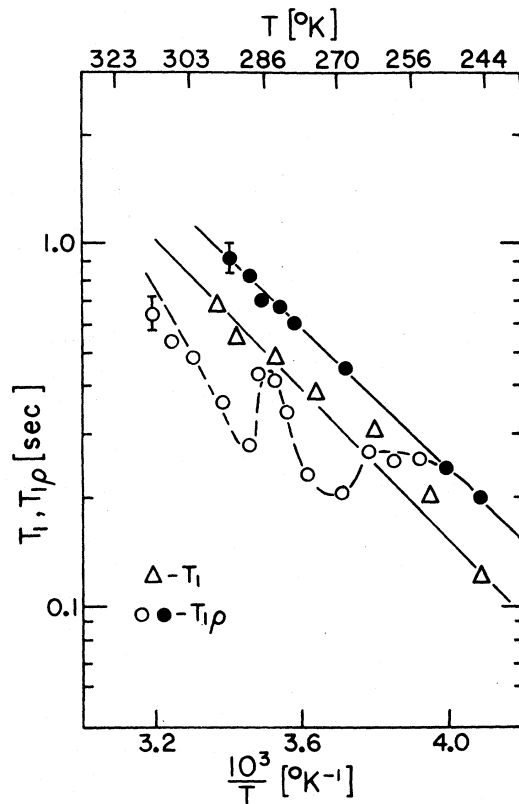


FIG. 3. Thermal structure in $T_{1\rho}$ in the vicinity of room temperature is shown by the open circles for an unannealed ADP sample, and shown by closed circles for the same sample after thermal annealing. The triangles indicate the T_1 values, which do not depend upon annealing treatments.

Moreover, after the sample is annealed a few hours at 320 °C, remeasurement of $T_{1\rho}$ (closed circles) shows that these minima have disappeared. Apparently during annealing the rapidly diffusing entities eventually find stable trapping sites where they are immobilized and subsequently do not contribute to $1/T_{1\rho}$ at lower temperatures. We note also that after these nonintrinsic effects are removed by annealing, the $T_{1\rho}$ values actually are longer than T_1 . The ratio is $T_1/T_{1\rho} \approx 0.8$; this surprising behavior was predicted (Sec. III C 4) for the contributions from two-fold hindered rotations of the ammonium ion.

Newman's cw saturation experiments¹⁴ for T_1 also showed a secondary minimum in the same temperature range where we have observed the nonintrinsic $T_{1\rho}$ minima. Saturation techniques measure a product of T_1 with a transverse relaxation time. Consequently, we speculate that the nonintrinsic $T_{1\rho}$ minima observed near room temperature are reflected in the cw saturation measurements, whereas they are not observed in the pulsed direct T_1 measurements.

In addition, much of the complex temperature dependence of the proton $T_{1\rho}$ relaxation observed by Grosescu²⁶ in ADA appears quite similar to the impurity-diffusion effects described above for ADP. From Fig. 3, we note that such nonintrinsic mechanisms can make large contributions to the observed $1/T_{1\rho}$. In our case, they contribute sharp temperature-dependent structures whose peak relaxation rates are 2–3 sec^{-1} above that for well-annealed ADP samples. We believe, therefore, that much of the qualitative difference between $T_{1\rho}$ behaviors in ADA and ADP samples can be attributed to similar impurity-related effects.

VI. PHASE TRANSITION ANOMALY

The rotating-frame relaxation rate shows a very large anomaly in $1/T_{1\rho}$ at the AFE transition temperature. Figure 4 presents the behavior of $1/T_{1\rho}$ and $1/T_1$ in the temperature range around the T_1 minimum and near the phase-transition temperature $T_c \approx 147$ °K. In the temperature range from 180 to 165 °K shown in Fig. 4, the NMR system is in an intermediate-correlation-time regime, and $1/T_1$ and $1/T_{1\rho}$ are very nearly equal. Most interesting, however, is the strong additional component contributing to $1/T_{1\rho}$. This becomes readily observable about 10 °K above T_c and increases rapidly as the temperature decreases approaching T_c .

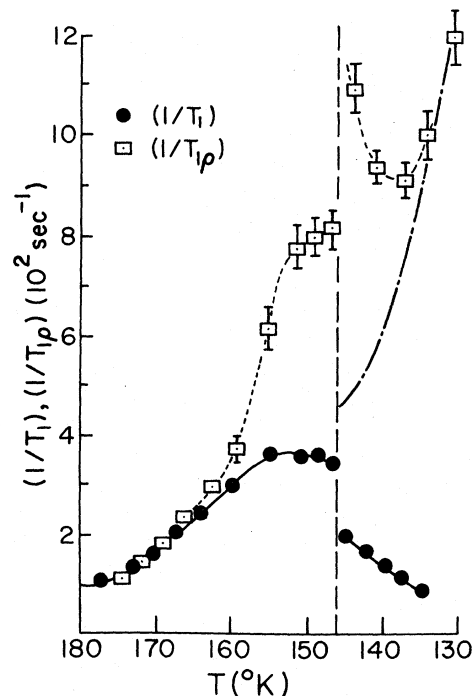


FIG. 4. Behavior of $1/T_1$ and $1/T_{1\rho}$ for temperatures in the vicinity of the ADP antiferroelectric phase transition.

Near 147 °K, the additional $1/T_{1\rho}$ component is at least $5 \times 10^2 \text{ sec}^{-1}$. This is an extremely large effect, more than 10^2 stronger than a similar "anomalous" contribution observed by Blinc *et al.*²⁷ in the proton $1/T_1$ behavior of dicalcium strontium propionate near its AFE phase transition.

To discuss further the behavior of the additional anomalous contribution to $1/T_{1\rho}$, which we call $(1/T_{1\rho})_A$, we adopt a rough approximation for subtracting the baseline contributions from ammonium-ion hindered rotations. The following approach seems to be a reasonably conservative one. First, at temperatures above T_c , where the ammonium rotational correlation times are not very large compared to $(\gamma H_0)^{-1}$, we know that the ammonium-ion rotation contribution to $1/T_{1\rho}$ is at most about equal to $1/T_1$. Therefore, we simply subtract the measured $1/T_1$ from the measured $1/T_{1\rho}$ to estimate the anomalous component,

$$(1/T_{1\rho})_A = 1/T_{1\rho} - 1/T_1, \quad T > T_c. \quad (15)$$

Second, for $T < T_c$, the rotational correlation times have abruptly lengthened to where $1/T_1$ is responding according to $\gamma H_0 \tau_r \gg 1$. In this limit, $1/T_{1\rho}$ has a continuing contribution directly from the $1/T_1$ mechanisms and also has a dominant contribution proportional to T_1 , as given by Eq. (6). The dashed-dotted line in Fig. 4 is a derived relaxation-rate contribution corresponding to Eq. (6). It is inversely proportional to the measured $1/T_1$ for $T < T_c$ and normalized to fit the $1/T_{1\rho}$ values below 140 °K. For $T < T_c$, we estimate $(1/T_{1\rho})_A$ by subtracting both the measured $1/T_1$ and the dash-dotted curve in Fig. 4 from the measured $1/T_{1\rho}$. The resulting behavior of $(1/T_{1\rho})_A$ is shown in Fig. 5.

We can attempt to interpret the $(1/T_{1\rho})_A$ anomaly in terms of the model of an unstable damped anti-ferroelectric lattice mode, which Blinc *et al.*²⁷ successfully apply to a weak $1/T_1$ anomaly observed in dicalcium strontium propionate. The results, however, are completely unsatisfactory; to give the observed $(1/T_{1\rho})_A$ magnitude, the mode frequency must slow to about 10^5 Hz with a damping time of at least 10^{-5} sec. These values, even for an unshattered sample, are physically unreasonable. Furthermore, the soft-mode model predicts, at slightly higher temperatures, a $1/T_1$ anomaly, but this is not experimentally observed. Finally, the observed temperature dependence for $T > T_c$ is far stronger than can be accounted for by the soft-mode model.

Neither can the observed $(1/T_{1\rho})_A$ be caused directly by some strong additional slowing of the individual ammonium-ion rotations. The required anomalous increase in the rotational correlation time would then be glaringly observed also in the $1/T_1$ data, but this is not seen experimentally.

Although the detailed relaxation process is not understood, the experimental NMR data can give estimated limits on the physical parameters governing the $1/T_{1\rho}$ anomaly near T_c . The $1/T_{1\rho}$ results in Fig. 5 can be viewed according to Eq. (7) where we suppose that τ increases rapidly as T decreases approaching T_c , and τ becomes very long for T less than T_c so that the field fluctuations become effectively frozen-in as a static effect. Thus a maximum value can be estimated for the h^2 term in Eq. (7) from local-field changes in the proton resonance as T decreases through T_c . Observation of the proton free-induction-decay, the $T_{1\rho}$ dependence upon H_1 , and the cw line-breadth measurements of others²⁵ show that only a small change, at most about 1 G^2 , occurs in the mean-squared local fields as the temperature passes through the phase transition. If we use this as an upper limit, $h^2 \leq 1 \text{ G}^2$, and employ the maximum $(1/T_{1\rho})_A$ values from Fig. 5, then Eq. (6) yields the estimate $\tau \leq 5 \times 10^{-7}$ sec for $T \approx T_c$.

The experiments described here used $(\gamma H_1)^{-1} = 6.2 \times 10^{-6}$ sec; so the above estimate gives $\tau < (\gamma H_1)^{-1}$, but shows that τ may be growing comparable to $(\gamma H_1)^{-1}$ near T_c . This appears to be consistent with the change in curvature of $(1/T_{1\rho})_A$ (see Fig. 5) as T decreases within a few degrees above T_c . This behavior may reflect an approach toward a $(1/T_{1\rho})_A$ maximum, which occurs according to Eq. (7) for $\tau \approx (\gamma H_1)^{-1}$. Consequently, it seems that the limits on the correlation time for $T \approx T_c$ are

$$6 \times 10^{-6} > \tau > 5 \times 10^{-7} \text{ sec.} \quad (16)$$

Such a large correlation time, together with its

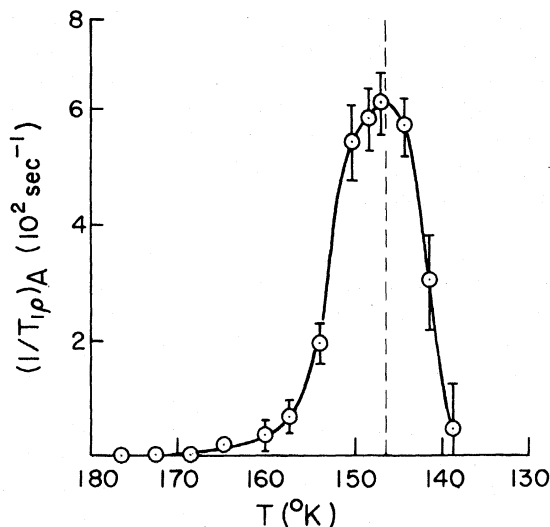


FIG. 5. Phase-transition anomalous contribution to $1/T_{1\rho}$. This is derived from the data of Fig. 4, as explained in the text.

extremely rapid decrease as T becomes greater than T_c , suggests that rather gross local ionic displacements and distortions are involved in the cooperative mechanisms underlying the ADP phase transition. This appears consistent with the independent evidence for strong ammonium-ion distortions occurring below T_c and with the crystallographic structure change which accompanies the AFE phase transition.

VII. SUMMARY

Over most of the temperature range from 320 to 77 °K, both the longitudinal relaxation rate $1/T_1$ and the rotating-frame relaxation rate $1/T_{1\rho}$ for protons in ADP are dominated by the intra-ammonium proton dipole-dipole interactions. These interactions fluctuate due to thermally-activated hindered rotations of the ammonium ions. Near the antiferroelectric-phase-transition temperature $T_c \approx 147$ °K, $1/T_1$ displays a smoothly varying temperature dependence and exhibits only a 50% discontinuity across T_c . No observable change in the shape of the NMR free-induction-decay signal occurs across T_c . On the other hand, a very strong and sharply temperature-dependent anomaly contributes to $1/T_{1\rho}$ at temperatures close to T_c . This anomaly adds to a smoothly varying baseline behavior of $1/T_{1\rho}$; the baseline $1/T_{1\rho}$ contribution may quantitatively be identified with the same ammonium-ion reorientation dynamics that give the observed $1/T_1$ behavior. These observations imply that the mechanisms producing the AFE transition only modestly perturb the ammonium-ion reorientation times, and the transition is not associated with a cooperative freezing-in of the molecular rotations.

The strong $1/T_{1\rho}$ anomaly at T_c , however, shows that one can observe by NMR the cooperative slowing and freezing-in of some dynamical mechanism associated with the AFE transition. The strength of the $1/T_{1\rho}$ anomaly, its sharp temperature dependence, the absence of any significant NMR line-breadth changes, and the absence of any corresponding anomaly in $1/T_1$ yield additional information:

(i) Whatever the exact nature of the dynamical mechanisms operating near T_c , they slow to very long correlation times, at least $\sim 10^{-6}$ sec, within a few degrees Kelvin above T_c , and freeze-in to an essentially static state within a few degrees below T_c .

(ii) The mean-squared field fluctuations by which these AFE transition mechanisms contribute to the proton NMR relaxation are small compared to the intra-ammonium proton interactions. Their strength is perhaps on the order of 1 G², comparable to a few tenths of the mean-squared dipolar interactions coupling the ammonium protons to

the hydrogen-bond protons and phosphorus nuclei.

(iii) The model of critical slowing of an overdamped quasi-spin-wave mode²⁷ has been used to describe NMR relaxation-rate anomalies in dicalcium strontium propionate. The anomalies we observe in ADP, however, are two orders of magnitude stronger and cannot physically be described by such a model.

In addition to results concerning the AFE phase-transition region, other findings from the $1/T_1$ and $1/T_{1\rho}$ ADP experiments appear significant. Temperature-dependent structures occurring in the $1/T_{1\rho}$ values around room temperatures may be removed by thermal annealing of the samples. These appear to be nonintrinsic and caused by the diffusion of impurities and defects in the material. They offer possible reasons for the differences in T_1 behavior, as observed by cw and by pulsed NMR techniques, and may explain the much greater thermal complexity of $T_{1\rho}$ behavior in ammonium dihydrogen arsenate as compared with that we observe ADP. In annealed samples, at high temperatures in the very-short-correlation-time regime, $T_{1\rho}$ is actually measured to be slightly longer than T_1 . Theoretical calculations yield this result only for the highly symmetric case of ammonium-ion reorientation about the ammonium-tetrahedron two-fold rotation axes.

Finally, above the AFE transition, no anisotropy is observed either for T_1 or for $T_{1\rho}$, depending upon whether the external magnetic field is aligned along the crystalline c axis or along the a (b) axis. Below the transition temperature in the AFE phase, however, a strong temperature-dependent anisotropy is observed in T_1 . Analysis of the data and theoretical calculations show that this behavior can be described by the following model: In the paraelectric phase, the a , b , and c -axis reorientation activation energies are all equal at 3.8 kcal/mole. Upon undergoing the AFE transition, the c -axis activation energy increases to 4.2 kcal/mole, while the a - (b)-axis activation energy decreases to 2.8 kcal/mole. In addition, to produce the anisotropy, the ammonium ion must be rather severely distorted in the AFE phase from its normal tetrahedral configuration; this supports evidence from previous ir measurements that strong ammonium-ion distortions occur below T_c .

APPENDIX

Theoretical expressions for $1/T_1$ and $1/T_{1\rho}$ contributions from intra-ammonium proton interactions due to hindered rotations are derived in detail by Kodama,²⁸ for the case of NH_4Cl . Complete details of the mathematical manipulations occur in Kodama's paper, so that we need present here only an outline of appropriate derivations. Unfortunately, Kodama's treatment employs 90°

reorientations, undistorted ammonium tetrahedra, and numerical evaluations are performed only for powder-average conditions. None of the conditions obtain for ADP. Genin and O'Reilly quote expressions for $1/T_1$ and $1/T_{1\rho}$ for the case of ferroelectric leptonite. In that material, reorientations occur about the ammonium-ion three-fold axes. The resulting expressions are the same form as for rotations about random axes through infinitesimal angles; as shown later in this Appendix, this occurs independent of ammonium-ion distortions. For our purposes, however, we must consider twofold rotations and explicitly treat the effect of tetragonal distortions of the ammonium tetrahedra.

We therefore begin with the fundamental relations given by Kodama,²⁸ or with a trivial extension of those given by Abragam²² for like-spin dipolar relaxation.

$$1/T_1 = \frac{3}{2} \gamma^4 \hbar^2 I(I+1) \times [J^{(1)}(\gamma H_0) + J^{(2)}(2\gamma H_0)], \quad (\text{A1})$$

and

$$1/T_{1\rho} = \frac{3}{2} \gamma^4 \hbar^2 I(I+1) \left[\frac{5}{2} J^{(1)}(\gamma H_0) + \frac{1}{4} J^{(2)}(2\gamma H_0) + \frac{1}{4} J^{(0)}(2\gamma H_1) \right], \quad (\text{A2})$$

where

$$J^{(a)}(\omega) = \int_{-\infty}^{\infty} \langle F^{(a)}(t) F^{(a)}(t+\tau) \rangle_t e^{i\omega\tau} d\tau. \quad (\text{A3})$$

The pair-wise interactions $F^{(a)}$ are

$$F^{(1)} = r^{-3} \sin\theta \cos\theta \cos\phi, \quad (\text{A4})$$

$$F^{(2)} = r^{-3} \sin^2\theta \cos(2\phi), \quad (\text{A5})$$

and

$$F^{(0)} = r^{-3} (1 - 3\cos^2\theta), \quad (\text{A6})$$

where θ and ϕ are the usual azimuthal and polar angles of the internuclear vector with respect to the direction of H_0 .

Abragam²² details the expansion of the rotational probability function in Legendre polynomials and calculates explicitly the case of reorientation by infinitesimal rotations. Precisely the same formalism can be used for finite rotation angles, with random reorientation jumps and is detailed by Kodama. The result gives the familiar form,

$$\langle F(t) F^*(t+\tau) \rangle_t = \langle \delta F^2 \rangle e^{-\tau/\tau}, \quad (\text{A7a})$$

and, from Eq. (A3)

$$J(\omega) = \langle \delta F^2 \rangle \tau [1 + (\omega\tau)^2]^{-1}, \quad (\text{A7b})$$

where $\langle \delta F^2 \rangle$ is the mean-squared fluctuation of the interaction occurring upon reorientation, and $1/\tau$ is the mean rate at which such reorientations occur.

Some general observations are helpful at this point. First, from Eq. (A1), if $\gamma H_0\tau \ll 1$, then $1/T_1$ is proportional to τ , as deduced from Eqs. (A7a), (A7b), and (A3). On the other hand, when $\gamma H_0\tau \gg 1$, then $1/T_1$ is proportional to $1/\tau$. The detailed behavior may be derived, but a very useful approximation is

$$1/T_1 = \frac{3}{2} \gamma^4 \hbar^2 I(I+1) \times \langle \delta F^{(1)2} \rangle \tau [1 + R(\gamma H_0\tau)^2]^{-1}, \quad (\text{A8})$$

where

$$R = 4 (\langle \delta F^{(1)2} \rangle + \langle \delta F^{(2)2} \rangle) (4 \langle \delta F^{(1)2} \rangle + \langle \delta F^{(2)2} \rangle)^{-1}. \quad (\text{A9})$$

Second, when $\gamma H_0\tau \ll 1$, both $1/T_1$ and $1/T_{1\rho}$ increase proportionally to τ , but when $\gamma H_0\tau \gg 1$ then the $J^{(0)}$ term in Eq. (A2) dominates. That is, $1/T_{1\rho}$ continues to grow proportionally to τ , unlike $1/T_1$, until $\gamma H_1\tau \approx 1$. Consequently, for any interactions in the limit $\gamma H_0\tau \gg 1$, $1/T_{1\rho}$ has the form

$$1/T_{1\rho} = (\gamma\hbar)^2 \tau [1 + (\gamma H_0)^2 \tau^2]^{-1}, \quad (\text{A10})$$

where H_ρ^2 is the rotating frame total mean-square effective field. For example, for the dipole pair interactions of Eq. (A6),

$$H_\rho^2 = (2H_1)^2 + H_L^2, \quad (\text{A11})$$

where H_L^2 is the residual, un-narrowed local-field second moment, and $H_\rho = 2H_1$ in the large H_1 limit.

We now consider the specific case of relaxation contribution from the intra-ammonium proton interactions. Although the ADP lattice has tetragonal symmetry in the PE state, we may start by assuming the ammonium-ion "tetrahedron" is not greatly distorted. Figure 6 shows the four proton positions, which we call *A*, *B*, *C*, and *D*, and their average orientation with respect to the ADP *a*, *b*, and *c* axes. First, we note the effect of rotations about the three-fold symmetry axes, i. e., where the rotation axes have directions $(\pm 1, \pm 1, \pm 1)$. The scalar products, $(\pm 1, \pm 1, \pm 1) \cdot \hat{a}$ (or \hat{b} or \hat{c}), are equal for all four three-fold rotations. Since the dipolar interactions in Eqs. (A4–A6) all depend upon the polar and azimuthal sines and cosines, the squares of their fluctuations are equivalent for any three-fold rotation. The same observation holds for reorientation about random axes [which may be expressed on the average as equivalent to $(\pm 1, \pm 1, \pm 1)$ rotations], as might occur in a liquid or gas. There are two consequences: First, $1/T_1$ and $1/T_{1\rho}$ are

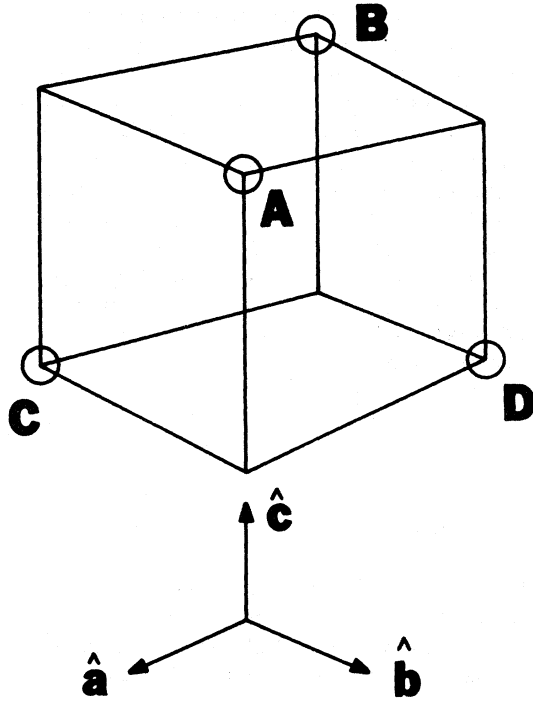


FIG. 6. Proton positions in the ammonium tetrahedron with respect to the crystalline axes in ADP.

equal in the short-correlation-time limit (as derived by Abragam), independent of whether the pair-wise proton interactions in the ammonium ion maintain perfect local tetrahedral symmetry in the tetragonal lattice. Second, since all three-fold rotations are equivalent with respect to the a , b , or c axes, $1/T_1$ should show no anisotropy for H_0 parallel to c compared with H_0 parallel to a or b . This agrees with the explicit expressions given by Genin and O'Reilly.²⁹

It is important that the same equivalence does not exist for the two-fold rotations, i. e., rotational axes in the $(1, 0, 0)$, $(0, 1, 0)$, or $(0, 0, 1)$ directions. The squared fluctuations for π -rotations about the a , b , and c axes (with mean independent rates $1/\tau_a$, $1/\tau_b$ and $1/\tau_c$, respectively) are listed in Table I for the three types of pairs, AB , AC , and AD , referenced in Fig. 6. Since $\cos^2\theta$ is invariant, for the tetrahedral interproton vectors under two-fold rotations, $J^{(0)}$ vanishes. Consequently, for the intra-ammonium tetrahedral terms, $1/T_1$ and $1/T_{1p}$ are proportional in both the long- and short-correlation-time limits. Also, in the absence of distortions, $r_{AC} = r_{AD} = r_{AB}$, so that the relative weighting of the $J^{(1)}$ and $J^{(2)}$ contributions, from Table I, is

$$J^{(1)}/J^{(2)} = 4 \times \frac{1}{4} / 2 \times 1 = \frac{1}{2}, \quad (\text{A12})$$

with

$$J^{(0)} = 0. \quad (\text{A13})$$

By substituting the relations in Eqs. (A12) and (A13) in Eqs. (A1) and (A2), we find $1/T_1 = 1/T_{1p}$ for $\gamma H_0 \tau \ll 1$ and perfect tetrahedral symmetry. Let us, however, consider the effect of tetragonal distortions appropriate to the PE phase ADP lattice. In particular, if r_{AB} is decreased by 5% from the average and r_{AC} and r_{AD} increased 5%, then r^6 changes drastically. In Table I the $(\delta F^{(2)})^2$ terms become a factor of 8 larger than the $(\delta F^{(1)})^2$ terms, rather than a factor of 4. This gives,

$$J^{(1)}/J^{(2)} = \frac{1}{4}, \quad (\text{A14})$$

in the short-correlation-time limit, and Eqs. (A1) and (A2) can be used to find the ratio

$$T_1/T_{1p} = 0.7. \quad (\text{A15})$$

TABLE I. Squared interaction fluctuations for two-fold rotations of ammonium tetrahedron corresponding to the proton-pair types AB , AC , and AD shown in Fig. 6. H_0 parallel to c axis.

	$\delta F^{(1)2}$			$\delta F^{(2)2}$			$\delta F^{(0)2}$		
	$r^{-6} \sin^2\theta \cos^2\theta \cos^2\phi$			$r^{-6} \sin^4\theta \cos^2(2\phi)$			$r^{-6} (1 - 3 \cos^2\theta)^2$		
π rotations	AB	AC	AD	AB	AC	AD	AB	AC	AD
	$\sin\theta$	θ changes by π		θ changes by π or		
	or				ϕ changes by π		θ changes from $\pi/4$ to $3\pi/4$		
	$\cos\theta$								
	zero								
τ_c	0	$\left(\frac{1}{4}\right) r_{AC}^{-6}$	$\left(\frac{1}{4}\right) r_{AD}^{-6}$	0	0	0	0	0	0
τ_a	0	$\left(\frac{1}{4}\right) r_{AC}^{-6}$	0	$(1) r_{AB}^{-6}$	0	0	0	0	0
τ_b	0	0	$\left(\frac{1}{4}\right) r_{AD}^{-6}$	$(1) r_{AB}^{-6}$	0	0	0	0	0

This distorted ammonium case also corresponds to a value of R in Eqs. (A8) and (A9) of

$$R = \frac{5}{2} \approx (1.6)^2. \quad (\text{A16})$$

We now consider anisotropy in $1/T_1$ in the AFE phase in the limit $\gamma H_0 \tau \gg 1$. From Table I, we have

$$1/T_1 \propto \frac{1}{4} r_{AC}^{-6} (1/\tau_c + 1/\tau_a) + \frac{1}{4} r_{AD}^{-6} (1/\tau_c + 1/\tau_b) + (1) r_{AB}^{-6} \frac{1}{4} (1/\tau_a + 1/\tau_b); \quad \vec{H}_0 \parallel \hat{c}. \quad (\text{A17})$$

When the sample is rotated to bring $\vec{H}_0 \parallel \hat{a}$, the results are obtained simply from Table I by interchanging the pairs AB and AC ,

$$1/T_1 \propto \frac{1}{4} r_{AB}^{-6} (1/\tau_c + 1/\tau_a) + \frac{1}{4} r_{AD}^{-6} (1/\tau_c + 1/\tau_b) + (1) r_{AC}^{-6} \frac{1}{4} (1/\tau_a + 1/\tau_b); \quad \vec{H}_0 \parallel \hat{a}. \quad (\text{A18})$$

We note, from Eqs. (A17) and (A18), that if $r_{AD} = r_{AB}$ or if $\tau_c = \tau_a = \tau_b$, then $(1/T_1 \vec{H}_0 \parallel \hat{a})$ and $(1/T_1 \vec{H}_0 \parallel \hat{c})$ are equal. We previously considered the effect of relative weak tetragonal distortions

in the PE phase. Infrared-absorption experiments⁹ imply very strong distortions occurring in the AFE phase. Because of the r^{-6} dependence, strong tetragonal distortions decreasing r_{AB} and increasing r_{AC} and r_{AD} can lead to total domination of the terms in r_{AB}^{-6} in Eqs. (A17) and (A18). Thus, Eq. (A17) would be dominated by $(1/\tau_a + 1/\tau_b) r_{AB}^{-6}$ and Eq. (A18), by $(1/\tau_c + 1/\tau_a) r_{AB}^{-6}$. To be precise, we should also include the CD pair (equivalent to AB), whose rotation rate corresponding to Eq. (A18) is $1/\tau_c + 1/\tau_b$. Then, for this strongly distorted case of relaxation domination by the AB and CD proton pairs,

$$1/T_1 \propto r_{AB}^{-6} (2/\tau_a + 2/\tau_b); \quad \vec{H}_0 \parallel \hat{c}, \quad (\text{A19})$$

whereas

$$1/T_1 \propto r_{AB}^{-6} (2/\tau_c + 1/\tau_a + 1/\tau_b); \quad \vec{H}_0 \parallel \hat{a}. \quad (\text{A20})$$

The conclusion from Eqs. (A19) and (A20) is that an anisotropy in $1/T_1$ requires both a strong ammonium-ion tetragonal distortion and strong tetragonal rotational asymmetries so that $2/\tau_c \neq (1/\tau_a) + (1/\tau_b)$.

*This work supported in part by the U.S. National Science Foundation, Division of Materials Research.

†Present address: Tata Institute of Fundamental Research, Homi Bhabha Road, Bombay 5, India.

¹R. Ueda, J. Phys. Soc. Jpn. **3**, 328 (1948).

²R. O. Keeling and R. Pepinsky, Z. Kristallogr. **196**, 236 (1955).

³Leon Tenzer, B. C. Frazer, and R. Pepinsky, Acta Cryst. **11**, 506 (1958).

⁴V. N. Kolomichuk, Kristallografiya **13**, 519 (1968) [Sov. Phys.—Crystallogr. **13**, 422 (1968)].

⁵E. A. Wood, W. J. Merz, and B. T. Matthias, Phys. Rev. **87**, 544 (1952).

⁶T. Nagamiya, Prog. Theor. Phys. **7**, 275 (1952).

⁷W. P. Mason and B. T. Matthias, Phys. Rev. **88**, 477 (1952).

⁸C. C. Stephenson and A. C. Zettlemyer, J. Am. Chem. Soc. **66**, 1405 (1944).

⁹E. Wiener-Avneer, S. Levin, and I. Pelah, J. Chem. Phys. **52**, 2891 (1970).

¹⁰G. A. Samara, Phys. Rev. Lett. **27**, 103 (1971).

¹¹G. A. Samara, J. Phys. Soc. Jpn. Suppl. **28**, 399 (1970).

¹²N. S. Dalal and C. A. McDowell, Phys. Rev. B **5**, 1074 (1971).

¹³R. Blinc, *Advances in Magnetic Resonance*, edited by John S. Waugh (Academic, New York, 1968), Vol. 3, p. 141.

¹⁴Roger Newman, J. Chem. Phys. **18**, 669 (1950).

¹⁵D. J. Genin, D. E. O'Reilly, and Tung Tsang, Phys. Rev. **167**, 445 (1968).

¹⁶Jerome Wagner, Ph.D. thesis (Univ. of Wisconsin, Madison, 1970) (unpublished).

¹⁷C. P. Slichter and D. Ailion, Phys. Rev. **135**, A1099 (1964).

¹⁸S. R. Kasturi and P. R. Moran, Bull. Am. Phys. Soc. **16**, 317 (1971).

¹⁹S. R. Kasturi, Ph.D. thesis (Univ. of Wisconsin, Madison, 1972) (unpublished).

²⁰D. C. Ailion and C. P. Slichter, Phys. Rev. **137**, A235 (1965).

²¹D. Ailion, Ph.D. thesis (Univ. of Illinois, 1964) (unpublished).

²²A. Abragam, *The Principles of Nuclear Magnetism* (Clarendon, Oxford, 1961), Chap. VIII.

²³D. E. O'Reilly and T. Tsang, J. Chem. Phys. **46**, 1291 (1967).

²⁴S. R. Miller, R. Blinc, M. Brenman, and J. S. Waugh, Phys. Rev. **126**, 528 (1962).

²⁵Guy J. Adriaenssens and John L. Bjorkstam, J. Chem. Phys. **55**, 1137 (1971).

²⁶R. Groseanu, Chem. P. Lett. **21**, 80 (1973).

²⁷R. Blinc, S. Zumer, and G. Lahajnar, Phys. Rev. B **1**, 4456 (1970).

²⁸T. Kodama, J. Mag. Res. **7**, 137 (1972).

²⁹D. J. Genin and D. E. O'Reilly, J. Chem. Phys. **50**, 2842 (1969).